

# Alt-MoE: A Scalable Framework for Bidirectional Multimodal Alignment and Efficient Knowledge Integration

Hongyang Lei<sup>1</sup>, Xiaolong Cheng<sup>1</sup>, Dan Wang<sup>1</sup>, Kun Fang<sup>1</sup>, Qi Qin<sup>2</sup>, Huazhen Huang<sup>3</sup>,  
Yetao Wu<sup>1</sup>, Qingqing Gu<sup>1</sup>, Zhonglin Jiang<sup>1</sup>, Yong Chen<sup>1</sup>, Luo Ji<sup>1\*</sup>

<sup>1</sup>Geely Automobile Research Institute (Ningbo) Co., Ltd

<sup>2</sup>Peking University

<sup>3</sup>Shenzhen Institute of Advanced Technology, CAS

## Abstract

*Multimodal learning has advanced significantly by aligning different modalities within shared latent spaces, enabling tasks such as cross modal understanding and generation. Current alignment strategies in multimodal learning primarily include direct alignment using pre-trained or unified encoders and single-directional alignment via modality-specific connectors. Direct alignment struggles to fully leverage rich intra-modal knowledge, often requiring extensive training data to achieve cross-modal representation. Meanwhile, single-directional alignment methods, despite leveraging pre-trained knowledge, restrict task adaptability and hinder the model’s ability to capture bidirectional relationships, leading to incomplete knowledge fusion and underutilization of complementary modality-specific information. To address these limitations, we introduce Alt-MoE, a scalable multimodal alignment framework that employs a mixture of experts (MoE) model as a multi-directional connector across modalities. By utilizing a sequential alternating one-way alignment strategy, Alt-MoE iteratively refines the model to achieve bidirectional alignment. Alt-MoE operates in latent space, enabling efficient vector pre-storage and real-time retrieval via MoE, optimizing large-scale data processing. Extensive empirical studies demonstrate that Alt-MoE achieves competitive performance on cross-modal retrieval and visual question answering by integrating diverse modality-specific knowledge, generalizing to unseen data, and easily scaling to new tasks and modalities through dynamic adjustment of MoE capacity and expert activation.*

## 1. Introduction

Achieving human-level intelligence, a central goal of Artificial General Intelligence (AGI), requires building hierar-

chical world models capable of abstract reasoning. These models enable agents to predict, plan, and reason about complex, multi-layered environments. Abstract reasoning, particularly in high-dimensional latent spaces, is crucial for cross-modal understanding and generation. It requires integrating diverse sources of information across multiple modalities to construct unified, high-level representations. These representations must transcend individual modalities, enabling models to capture complex, abstract relationships [8, 22].

However, current multimodal learning often fall short in effectively capturing and utilizing this abstract reasoning across modalities. Current multimodal learning frameworks often rely on two primary strategies for aligning modalities: *direct alignment* using pre-trained or unified multimodal encoders and *single-directional alignment* through modality-specific connectors. Direct alignment methods, such as CLIP [37] and ImageBind [13], involve aligning modalities by mapping them into a shared space using pre-trained encoders. VLMo [4] and ONE-PEACE [40] utilize a unified multimodal encoder to integrate and model interactions across different modalities. On the other hand, single-directional alignment strategies, like BLIP-2 [25] and LLaVA [33], focus on connecting specific modalities through specialized components or connectors, often operating in a one-way alignment direction. These approaches aim to establish coherent cross-modal representations, but each comes with its limitations in capturing the full complexity of multimodal relationships.

Direct alignment of multiple encoders excel in generalization, and efficient cross-modal retrieval [13, 25, 42, 47]. Unified multimodal encoder facilitates deeper interactions across modalities and is particularly advantageous in scenarios requiring joint reasoning and holistic understanding [4, 40, 41]. Nevertheless, both approaches share limitations: they often miss fine-grained intra-modal details, struggle with tasks that demand abstract reasoning, and rely heavily

\*Corresponding author: Luo.Jil@geely.com

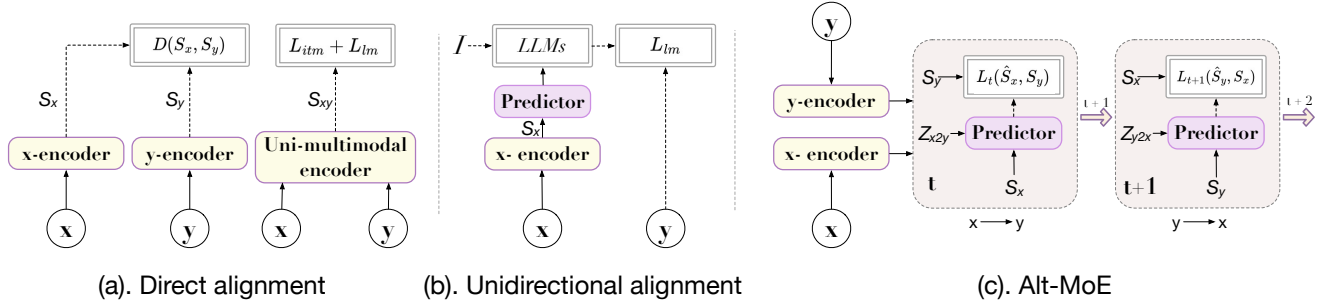


Figure 1. Primary strategies for aligning modalities: **Figure (a). Direct Alignment Framework:** This framework illustrates two types of alignment. On the left, a dual-encoder approach is shown, where an x-encoder and a y-encoder independently process inputs  $x$  and  $y$ , producing representations  $s_x$  and  $s_y$ . A similarity function  $D(s_x, s_y)$  is used to align the two modalities directly. On the right, a unified multimodal encoder jointly processes  $x$  and  $y$ , producing a fused representation  $s_{xy}$ . The training objective combines two loss functions:  $L_{itm}$ , focusing on image-text matching, and  $L_{lm}$ , which corresponds to the language modeling loss. **Figure (b). Unidirectional Alignment Framework:** In this framework, an x-encoder processes input  $x$  to produce a representation  $s_x$ , which is then refined by a predictor.  $I$  provides additional information to guide the predictor in aligning refined representations with a large language model (LLM). The LLM is trained with the language modeling loss  $L_{lm}$ , using input  $y$  as the target. This framework focuses on aligning the modality  $x$  unidirectionally to the language modality through the LLM. **Figure (c). Alt-MoE** models cross-modal bidirectional alignment by alternately executing unidirectional alignment tasks in the latent space (detail in 4.3).  $s_x, s_y$  represent the encoding results of the x-encoder and y-encoder, respectively.  $t, t + 1$  represent the time steps.  $L$  denotes the loss function (prediction and contrastive loss).  $z_{x2y}$  and  $z_{y2x}$  represent the cross embeddings (detail in 4.3).

on large-scale pre-training data. In text-guided visual representation learning, captions offer an abstract view of images, often missing pixel-level details crucial for complex visual reasoning. This limitation challenges direct alignment methods in retaining fine-grained intra-modal features, restricting their deep visual understanding capabilities [35].

Another method employs *single-directional alignment* through modality-specific connectors, such as LLaVA [33] and BLIP-2 [26]. These methods connect different modalities via specialized components, aligning them in a single direction. While this approach facilitates efficient cross-modal interaction and preserves unimodal richness, it can limit the model’s ability to capture complex, bidirectional relationships necessary for abstract reasoning. As a result, while it excels in specific tasks, it may struggle with more intricate, abstract reasoning that requires deeper intermodal dependencies.

Building upon these observations, we introduce **Alt-MoE**, a novel multi-modal alignment framework. Alt-MoE employs a unified, multi-directional MoE as cross-modal connector, enabling any-to-any modality alignment. This framework integrates the rich intra-modal knowledge of pre-trained models, preventing the loss of fine-grained information while avoiding high computational costs and data requirements. By employing Alternating Gradient Descent (AGD), bidirectional alignment decomposes into alternating unidirectional tasks, ultimately achieving bidirectional alignment. This method not only mitigates the risks of incomplete information and abstract reasoning deficien-

cies inherent in single-directional alignment but also allows the model to incorporate multiple loss functions, achieving more robust cross-modal alignment. Alt-MoE introduces a paradigm shift by exploring latent dependencies, enabling more dynamic and abstract forms of reasoning.

Further expanding on this, Alt-MoE is a new multi-modal paradigm which studies the dependency of the unobserved part ( $y$ ) on the observed part ( $x$ ) in their latent space. This enables the model to explore different hypothetical scenarios, plan actions, or make inferences about unobserved parts of the world based on observed data, thus facilitating more sophisticated and generalized reasoning. Experts within the MoE can operate at different levels of abstraction, ensuring that each modality is processed in a way that suits its nature while maintaining coherence in the overall model.

To assess the model’s performance, we achieved superior results across multiple tasks (e.g., VQA, image-text retrieval, audio-text retrieval, image classification) and datasets. Additionally, we validated the model’s generalization on unseen data by testing its performance on zero-shot audio-text retrieval. Experimental results demonstrate that our Alt-MoE easily achieves modality and task scaling while attaining competitive results compared to current state-of-the-art (SoTA) multi-modal studies. Furthermore, our approach is able to conduct large-scale on-line multi-modal retrieval tasks due to our unique architecture. We summarize our contributions as follows:

1. Alt-MoE introduces a modality-agnostic alignment method that reduces training and data costs while lever-

aging the rich knowledge in pre-trained models. This approach offers a new framework for multi-modal research, potentially enhancing efficiency and scalability across diverse modalities.

2. Alt-MoE leverages multi-directional MoE for cross-modal alignment in latent space, building a hierarchical world model that abstracts complex dependencies.

## 2. Related Works

### 2.1. End-to-end Multi-modal Learning

Recently, end-to-end multi-modal models employing various architectures have achieved outstanding performance. These architectures can be broadly categorized into several main types: Dual-encoder [18, 37], unified-encoder [6, 18, 27]. Combining dual encoder and fusion encoder architectures integrate specialized layers into multi-modal models to enable deep cross-modal interactions [24, 25].

The majority of multi-modal learning methods employ large-scale multi-modal datasets for end-to-end pre-training. However, as model scale continues to increase, several potential challenges emerge: Firstly, the pre-training process may incur prohibitively high computational costs. Secondly, these models often struggle to adapt to novel modalities or tasks without extensive re-training. Moreover, most multi-modal approaches employ text-guided learning of visual concepts, which can limit the acquisition of fine-grained information inherent to each modality. A logical approach is to leverage existing pre-trained uni-modal foundation models [26, 35, 45].

### 2.2. Multi-modal Learning with Uni-modal Models

Recent trends in multi-modal learning have increasingly focused on integrating high-performance uni-modal models to achieve multi-modal alignment. Flamingo [2] integrates visual information into each layer of a frozen Large LLM through the use of cross-attention. BLIP-2 [26] introduces an additional vision-to-language adaptation module, Q-former, and proposes a two-stage training process to mitigate the challenges associated with learning vision-language alignment. However, both methods require substantial parameters and multi-modal data for cross-modal alignment.

Recent studies indicate a convergence of representations across modalities, providing evidence for the feasibility of developing advanced multi-modal models by connecting high-performance uni-modal models with lightweight parameters and data-efficient techniques [16]. For instance, LLaVA [33] achieved state-of-the-art performance by employing a two-layer multilayer perceptron (MLP). Similar architectures have subsequently proliferated across various domains [23, 29, 30, 45]. Alt-MoE further advances this concept by interconnecting diverse high-performance

uni-modal models through a shared multi-directional MoE. We conducted extensive experiments focused on alignment efficacy, demonstrating the effectiveness of joint training across multiple modalities and directions.

### 2.3. Multi-modal Learning with MoE and AGD

Prior studies have investigated AGD-based multi-modal multi-task alternating training, revealing that the integration of diverse modalities, tasks, and resolutions can yield mutual benefits, thereby effectively enhancing the model’s generalization capabilities and cross-domain performance [1, 28]. We further extend this approach to integrate existing pre-trained high-performance uni-modal models, achieving overall alignment through alternating bidirectional alignment.

MoE-LLaVA [30] proposes MoE-Tuning, a strategy for Large Vision-Language Models that creates a sparse model with constant computational cost. While both MoE-LLaVA and Alt-MoE employ sparse MoE to connect high-performance uni-modal large models, Alt-MoE not only scales this approach to large audio-visual-language models but also achieves pairwise bidirectional alignment across modalities.

## 3. Problem Formulation

In this section, we first introduce the overall optimization objective of bidirectional alignment, followed by the optimization objective of unidirectional alignment, and finally the alignment loss and theoretical explanation. To clearly articulate the design rationale, we illustrate this with the example of image-text alignment.

1. Multi-modal alignment objective: Alt-MoE decomposes multi-modal bidirectional alignment into multiple unidirectional alignment subtasks, where MoE serves as a cross modal knowledge representation and fusion module and achieve multi-modal alignment by alternately aligning from image to text and text to image.
2. Alternating unidirectional alignment: Alt-MoE maximizes mutual information and minimizes conditional entropy to obtain independent and shared information for unidirectional alignment. Specifically, Alt-MoE adds embeddings as prior information to the input representations to guide the MoE in performing different pre-training tasks.
3. Information Decomposition and Alignment: we provide an information-theoretic explanation to elucidate the rationale behind the design of the training objective.

### 3.1. Multi-modal Alignment objective:

In this section, we will introduce the decomposition of the multi-modal bidirectional alignment objective. multi-modal alignment aims to align diverse modalities in a latent space

by finding optimal parameters  $\theta$  that minimize an alignment loss  $\mathcal{L}_{align}$ . This can be formulated as:

$$\theta^* = \arg \min_{\theta} \mathcal{L}_{align}(\theta). \quad (1)$$

By combining MoE  $f_{\theta}(\cdot)$  parameterized by  $\theta$  and AGD, which can decompose the optimization objectives for multi-modal alignment  $\mathcal{L}_{align}$  into multiple unidirectional alignment subtasks, and then alternately execute each subtask at various time step to achieve overall alignment. Specifically, the image-text alignment can be decomposed as follows in the following Equation 2:

$$\begin{aligned} \mathcal{L}_{i \rightarrow t}(\theta) &= \mathcal{L}_{i \rightarrow t}(\theta_{i \rightarrow t}) \oplus \mathcal{L}_{t \rightarrow i}(\theta_{t \rightarrow i}), \\ \theta &= \theta_{i \rightarrow t} \cup \theta_{t \rightarrow i}, \end{aligned} \quad (2)$$

where  $\mathcal{L}_{i \rightarrow t}, \theta_{i \rightarrow t}$  represents the image-to-text ( $t \rightarrow i$ ) alignment objective and parameter subset,  $\mathcal{L}_{t \rightarrow i}, \theta_{t \rightarrow i}$  represents the text-to-image ( $i \rightarrow t$ ) alignment objective and parameter subset,  $\oplus$  denotes an alternating optimization operation at various time step. Therefore, we decompose the image-text alignment into multiple unidirectional alignment optimizations and parameter subsets.

### 3.2. Alternating Unidirectional Alignment

In this section, we delineate the optimization objectives and parameter update procedures across various time steps  $t$ . By introducing AGD, we can alternately optimize unidirectional alignment at each time step  $t$  with the goals of maximizing mutual information between image  $I$  and text  $T$ , denoted as  $I(I; T)$ , and minimizing conditional entropies, denoted as  $H(T|I)$  and  $H(I|T)$ . The details of the multi-directional MoE are provided in the supplementary materials.

Given time step  $t$ , the objective function is updated as Equation 3:

$$\mathcal{L}_{i \rightarrow t} = \begin{cases} \mathcal{L}_{i \rightarrow t}^{(t)} = -I(I; T) + H(T|I), & \text{if } t = 2k \\ \mathcal{L}_{t \rightarrow i}^{(t)} = -I(I; T) + H(I|T), & \text{if } t = 2k + 1, \end{cases} \quad (3)$$

where  $k$  is a non-negative integer. Based on Equation 1 and 3, the overall optimization objective can be formulated as shown in Equation 4:

$$\theta^* = \arg \min_{\theta} (-I(I; T) + \lambda (H(T|I) + H(I|T))), \quad (4)$$

where  $\lambda$  is a weight parameter.

Given a set of parameters  $\theta$ , we alternate between image-to-text and text-to-image unidirectional alignment at different time steps. At different time steps, we update only a subset of the parameters:  $\theta_{i \rightarrow t}$  for  $i \rightarrow t$  alignment and  $\theta_{t \rightarrow i}$  for  $t \rightarrow i$  alignment. Ultimately, this process ensures that all parameters are updated, such that  $\theta = \theta_{i \rightarrow t} \cup \theta_{t \rightarrow i}$ .

The overall update process can then be described by the following Equation 5:

$$\theta^{t+1} = \begin{cases} \theta^t - \eta \nabla_{\theta_{i \rightarrow t}^t} \mathcal{L}_{i \rightarrow t}^{(t)}, & \text{if } t = 2k \\ \theta^t - \eta \nabla_{\theta_{t \rightarrow i}^t} \mathcal{L}_{t \rightarrow i}^{(t)}, & \text{if } t = 2k + 1, \end{cases} \quad (5)$$

where  $\eta$  is the learning rate,  $k$  is a non-negative integer.

### 3.3. Information Decomposition and Alignment

For image to text alignment, conditional entropy  $H(T|I)$  and  $H(I|T)$  represent modality-specific information in text and image respectively, measuring uncertainty in one modality after observing the other. Mutual information  $I(T; I)$  quantifies shared information between image and text modalities, indicating how much knowing one reduces uncertainty about the other. For accurate image-text alignment, high mutual information (more shared content) and low conditional entropy (less modality-specific information) are desirable, ensuring strong semantic coupling between modalities.

Alt-MoE leverages the MoE router to automatically select different experts, optimizing for these two objectives. This approach helps decouple modality-specific information from shared information, potentially improving the balance between capturing unique modal features and cross-modal relationships.

## 4. Methodology

In this section, we take image-text alignment as an example to provide a detailed introduction to the architecture of Alt-MoE. As shown in Figure 2, Alt-MoE is divided into three modules: the visual model (VM), the language model (LM), and the bidirectional alignment module MoE. We input the paired images and text ( $I, T$ ) into VM and LM respectively to obtain latent representations  $z_i, z_t$ , and then perform multi-modal interaction in the fusion module.

### 4.1. Image and Text Encoding

Given a pair of image and text inputs ( $I, T$ ), we employ separate encoders to process each modality. The visual model (VM)  $f_v(\cdot)$  encode the image  $I$ , while the language model (LM)  $f_l(\cdot)$  encode the text  $T$ . This process results in latent representations  $z_i$  and  $z_t$  for the image and text, respectively. The encoding can be formally expressed as:

$$\begin{aligned} z_i &= f_v(I), & z_i &\in \mathbb{R}^i, \\ z_t &= f_l(T), & z_t &\in \mathbb{R}^t, \end{aligned} \quad (6)$$

where  $z_i \in \mathbb{R}^i$  is the image representation, and  $z_t \in \mathbb{R}^t$  is the text representation.

### 4.2. Image and Text Encoding

Given a pair of image and text inputs ( $I, T$ ), we employ separate encoders to process each modality. The visual model

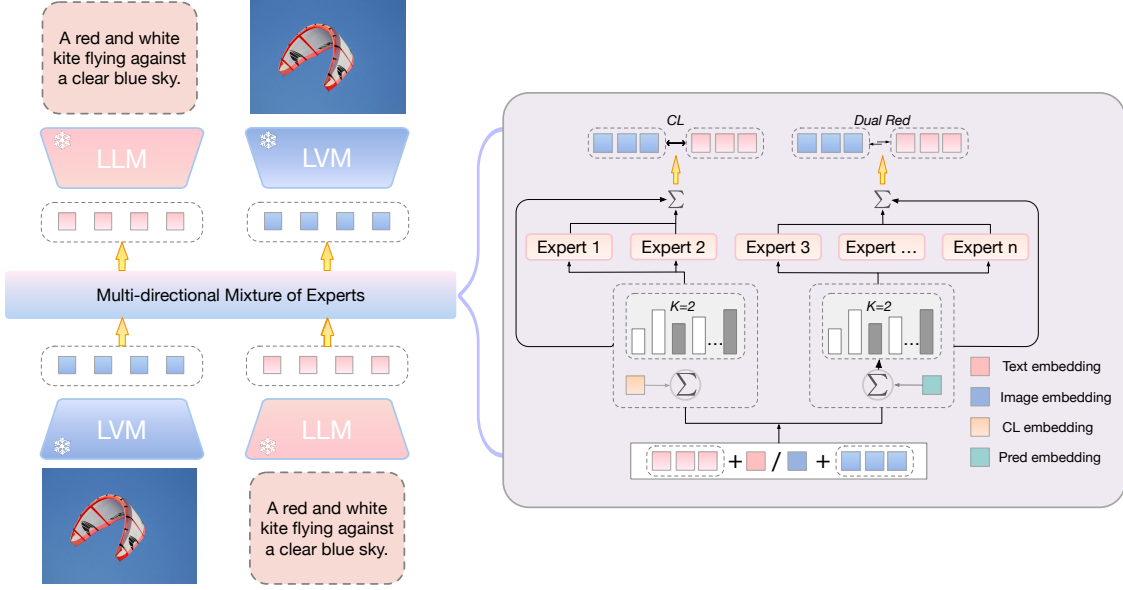


Figure 2. Overview of Alt-MoE: Alt-MoE connects different modalities through multi-directional MoE and performs unidirectional alignment from image to text and text to image at different time steps, ultimately achieving overall bi-directional alignment. Here, we take image-text alignment as an example. The left part of the figure illustrates the process of image-text alignment, where we alternately perform image-to-text and text-to-image alignment on a unified multi-directional MoE. The specific structure of the multi-directional MoE is shown in the figure on the right. Different embeddings prompt the MoE to select different experts to perform contrastive learning or prediction. *CL* refers to Contrastive Learning, and *Dual Pred* denotes Bidirectional Prediction. To guide the MoE in performing different sub-tasks, we introduce modality embeddings (e.g., text embeddings, image embeddings). These embeddings are incorporated through cross-embedding mechanisms to effectively steer the tasks.

(VM)  $f_v(\cdot)$  encode the image  $I$ , while the language model (LM)  $f_l(\cdot)$  encode the text  $T$ . This process results in latent representations  $z_i$  and  $z_t$  for the image and text, respectively. The encoding can be formally expressed as:

$$\begin{aligned} z_i &= f_v(I), & z_i &\in \mathbb{R}^i, \\ z_t &= f_l(T), & z_t &\in \mathbb{R}^t, \end{aligned} \quad (7)$$

where  $z_i \in \mathbb{R}^i$  is the image representation, and  $z_t \in \mathbb{R}^t$  is the text representation.

### 4.3. Unidirectional Alignment

At different time steps  $t$ , Alt-MoE performs unidirectional alignment tasks using different parameter updates and optimization objectives according to Equations 3 and 5. To guide MoE in selecting different experts for different modalities and tasks, we set up trainable modality encodings  $E_T, E_I$  and trainable task encodings  $E_{ce}, E_{mi}$ . Figure 3 illustrates the cross embedding process, where these embeddings are combined and added to  $z_t, z_i$  to guide the execution of different tasks. Specifically, we add modality embeddings to the input space  $z_i, z_t$  to enable the fusion module MoE to perceive the input modality, and then linearly project it into the  $d$ -dimensional common space  $z^c$  as

$$\begin{array}{lcl} E_{ce} & \longrightarrow & E_I \longrightarrow E_{ce} + E_I, E_{mi} + E_I \\ & \searrow & \nearrow \\ E_{mi} & \longrightarrow & E_T \longrightarrow E_{ce} + E_T, E_{mi} + E_T \end{array}$$

Figure 3. Cross Embedding.

follows:

$$z_i^c = W_i^1 \cdot z_i, \quad z_t^c = W_t^1 \cdot z_t, \quad z_i^c, z_t^c \in \mathbb{R}^d \quad (8)$$

where  $W_i^1 \in \mathbb{R}^{d \times i}$  and  $W_t^1 \in \mathbb{R}^{d \times t}$  are learnable projection matrices,  $d_i$  and  $d_t$  are the dimensions of the original image and text feature spaces respectively, and  $d$  is the dimension of the common space.

In the common latent space  $z^c$  with consistent dimensions, we update the loss function  $\mathcal{L}_{i \rightarrow t}, \mathcal{L}_{t \rightarrow i}$  at different time steps  $t$  according to Equation 5. We add different task embeddings to  $z^c$  to enable the MoE  $f_\theta(\cdot)$  to perceive tasks. Then, at different time steps  $t$ , we perform prediction and contrastive learning between image and text to maximize mutual information and minimize conditional entropy. Here, we take image-text alignment as an example; the same applies to text-audio alignment. This process alternates between image-to-text and text-to-image tasks as follows:

For image-to-text (at even time steps  $2k$ ):

$$\mathcal{L}_{i \rightarrow t} = \mathcal{L}_{\text{CE}}(\hat{z}_t, z_t) + \mathcal{L}_{\text{MI}}(z_i^{\text{mi}}, z_t),$$

where:

$$\begin{aligned} \hat{z}_t &= W^1 \cdot f_{\theta_{i \rightarrow t}}^1(z_i^c + E_{\text{ce}}), \\ z_i^{\text{mi}} &= W^2 \cdot f_{\theta_{i \rightarrow t}}^2(z_i^c + E_{\text{mi}}), \\ f_{\theta_{i \rightarrow t}} &= f_{\theta_{i \rightarrow t}}^1 \cup f_{\theta_{i \rightarrow t}}^2, \end{aligned} \quad (9)$$

where  $W^1 \in \mathbb{R}^{d \times t}$ ,  $W^2 \in \mathbb{R}^{d \times t}$  is a learnable projection matrix that map the output to dimensions consistent with  $z_t$ .

For text-to-image (at odd time steps  $2k + 1$ ):

$$\mathcal{L}_{t \rightarrow i} = \mathcal{L}_{\text{CE}}(\hat{z}_i, z_i) + \mathcal{L}_{\text{MI}}(z_t^{\text{mi}}, z_i),$$

where:

$$\begin{aligned} \hat{z}_i &= W_t^2 \cdot f_{\theta_{t \rightarrow i}}^1(z_t^c + E_{\text{ce}}), \\ z_t^{\text{mi}} &= W_t^2 \cdot f_{\theta_{t \rightarrow i}}^2(z_t^c + E_{\text{mi}}), \\ f_{\theta_{t \rightarrow i}} &= f_{\theta_{t \rightarrow i}}^1 \cup f_{\theta_{t \rightarrow i}}^2, \end{aligned} \quad (10)$$

where  $W^3 \in \mathbb{R}^{d \times i}$ ,  $W^4 \in \mathbb{R}^{d \times i}$  is a learnable projection matrix that map the output to dimensions consistent with  $z_i$ .

#### 4.4. Loss Function

We adopt a unidirectional prediction approach at each time step to minimize conditional entropy. This method involves predicting either text features from image features or image features from text features, alternating between time steps. We define the prediction loss function using the  $L2$  distance as follows:

$$\mathcal{L}_{\text{CE}} = |\hat{z}_t - z_t|_2^2 + |\hat{z}_i - z_i|_2^2, \quad (11)$$

where  $|\cdot|_2^2$  denotes the squared  $L2$  norm.  $\hat{z}_t$  and  $\hat{z}_i$  are the predicted text and image features, respectively, and  $z_t$  and  $z_i$  are the corresponding target features. At each time step, only one of these terms is active, depending on the prediction direction.

Here, we set  $z_t^{\text{mi}}$  as  $z^T$  and  $z_i^{\text{mi}}$  as  $z^I$  and contrastive loss can be formulated as follows:

$$\mathcal{L}_{\text{MI}} = \frac{1}{2N} \sum_{i=1}^N \left[ -\log \frac{\exp(\text{sim}(z_i^I, z_i^T)/\tau)}{\sum_{j=1}^N \exp(\text{sim}(z_i^I, z_j^T)/\tau)} - \log \frac{\exp(\text{sim}(z_i^T, z_i^I)/\tau)}{\sum_{j=1}^N \exp(\text{sim}(z_i^T, z_j^I)/\tau)} \right] \quad (12)$$

where:

- $N$  is the number of image-text pairs in a batch.
- $z_i^I$  and  $z_i^T$  are the latent representations of the  $i$ -th image and its corresponding text, respectively.
- $\text{sim}(z_i^I, z_j^T)$  is the cosine similarity between the latent representations  $z_i^I$  and  $z_j^T$ .
- $\tau$  is a temperature parameter that controls the sharpness of the similarity distribution.

## 5. Experiments and Results

We report Alt-MoE’s performance across various tasks, including image-text retrieval, speech-text retrieval, visual question answering, visual reasoning, and image classification on multiple datasets. Additionally, we validate Alt-MoE’s generalization capability on unseen data through zero-shot speech-text retrieval experiments. In the ablation study, we validated the impact of different Alt-MoE components through experiments on image-text retrieval tasks.

### 5.1. Datasets

The dataset details are provided in the supplementary materials. **Image-text retrieval:** COCO [31], Flickr30K [36]. **Zero-shot audio-text retrieval:** Clotho [11], Audiotapes [20]. **VQA:** VQA v2 [3], NLVR-2 [38]. **Image Classification:** ImageNet 1k [9].

### 5.2. Image-text Retrieval

Alt-MoE connects two uni-modal models through a multi-directional MoE, we train the multi-directional MoE on the COCO and Flickr30K, and then test it on the test sets. Table 1 shows the results of Alt-MoE on COCO and Flickr30K by integrating different LLMs such as LLAMA3-8b and Qwen2-7B with the LVMs Dinov2-Large. The results indicate that by integrating existing high-performance uni-modal models, Alt-MoE achieves superior performance.

Furthermore, by comparing different architectures of multi-modal models, Alt-MoE demonstrates superior data efficiency and parameter efficiency. Specifically, Alt-MoE has only 140M trainable parameters, which is significantly smaller than BLIP-2’s 1.2B trainable parameters.

The outstanding retrieval performance primarily stems from the MoE’s ability to capture abstract relationships across modalities through its diverse experts. Each expert specializes in particular high-level features, such as aligning the semantic content of an image with the semantic meaning of its textual description. This capability allows the model to reason beyond surface-level similarity, enabling it to uncover deeper patterns and themes within the data.

Additionally, cross-modal tasks often demand an understanding of data at multiple levels of granularity. The MoE architecture is inherently suited for hierarchical processing, with different experts focusing on varying levels of representation (e.g., object-level details in images or sentence-level semantics in text). This hierarchical modeling facilitates the construction of a structured world model, enhancing the model’s capacity for reasoning and aligning complex multimodal data effectively.

### 5.3. Zero-shot Audio-text Retrieval

To evaluate the model’s generalization ability on unseen data as well as its scalability across modalities and tasks,

Model	# Trainable Params	Flickr30K (1K test set)						COCO Fine-tuned (5K test set)					
		Image → Text			Text → Image			Image → Text			Text → Image		
		R@1	R@5	R@10	R@1	R@5	R@10	R@1	R@5	R@10	R@1	R@5	R@10
<i>Dual-encoder models</i>													
CLIP [37]	428M	88.0	98.7	99.4	68.7	90.6	95.2	-	-	-	-	-	-
ALIGN [7]	820M	88.6	98.7	99.7	75.7	93.8	96.8	77.0	93.5	96.9	59.9	83.3	89.8
FILIP [42]	417M	89.8	99.2	99.8	75.0	93.4	96.3	78.9	94.4	97.4	61.2	84.3	90.6
Florence [44]	893M	90.9	99.1	-	76.7	93.6	-	81.8	95.2	-	63.2	85.7	-
BEIT-3 [41]	1.9B	94.9	99.9	100.0	81.5	95.6	97.8	84.8	96.5	98.3	67.2	87.7	92.8
<i>Fusion-encoder models</i>													
UNITER [6]	303M	83.6	95.7	97.7	68.7	89.2	93.9	65.7	88.6	93.8	52.9	79.9	88.0
OSCAR [27]	345M	-	-	-	-	-	-	70.0	91.1	95.5	54.0	80.8	88.5
VinVL [46]	345M	-	-	-	-	-	-	75.4	92.9	96.2	58.8	83.5	90.3
<i>Dual encoder + Fusion encoder</i>													
ALBEF [24]	233M	94.1	99.5	99.7	82.8	96.3	98.1	77.6	94.3	97.2	60.7	84.3	90.5
BLIP [25]	446M	97.1	100.0	100.0	86.7	97.3	98.7	82.4	95.4	97.9	65.1	86.3	91.8
BLIP-2 ViT-L [26]	474M	96.9	100.0	100.0	88.6	97.6	98.9	83.5	96.0	98.0	66.3	86.5	91.8
BLIP-2 ViT-g [26]	1.2B	97.6	100.0	100.0	89.7	98.1	98.9	85.4	97.0	98.5	68.3	87.7	92.6
<i>LLMs + LVMs</i>													
Alt-MoE (LLaMA3-8b, DinoV2-L)	140M	97.8	<b>100.0</b>	<b>100.0</b>	<b>97.8</b>	<b>100.0</b>	<b>100.0</b>	87.7	<b>99.6</b>	<b>99.9</b>	89.7	<b>99.7</b>	<b>99.9</b>
Alt-MoE (Qwen2-7b, DinoV2-L)	130M	<b>97.9</b>	<b>100.0</b>	<b>100.0</b>	<b>97.8</b>	<b>100.0</b>	<b>100.0</b>	<b>88.1</b>	99.4	99.8	<b>90.1</b>	99.6	<b>99.9</b>

Table 1. Comparison with state-of-the-art image-text retrieval methods, finetuned on COCO and Flickr30K.

we validated Alt-MoE through zero-shot audio-to-text retrieval experiments. Specifically, we trained Alt-MoE on a pretraining dataset and validated its performance on Clotho and Audiotocaps, using the same architecture as in image-text retrieval. Details of the pretraining data are provided in the supplementary materials.

As shown in the table 2, Alt-MoE demonstrates superior performance over baseline models in zero-shot retrieval tasks, showcasing its exceptional generalization capabilities. This is primarily due to two key factors: first, the model benefits from the rich intra-modal knowledge embedded in pre-trained uni-modal models, which allows it to leverage existing knowledge without the need for extensive retraining. Second, the hierarchical MoE structure significantly strengthens abstract reasoning abilities. MoE models are known to excel at capturing complex, high-level patterns by assigning specialized experts to different levels of abstraction. This structured, layered processing enables Alt-MoE to model intricate relationships between modalities, further improving its ability to generalize and make inferences based on unseen data.

MoE significantly enhances abstract reasoning by assigning specialized experts to different levels of abstraction. This allows Alt-MoE to capture complex, high-level patterns and model the intricate relationships between modalities. Such a structure improves the model’s generalization ability and inference capabilities on unseen data.

## 5.4. Visual Question Answer

Visual Question Answering (VQA) is a challenging task that demands our visual language model to integrate an image with relevant questions to provide accurate responses.

Our experiments are conducted on the VQAv2 dataset [14], where each image is associated with several question-answer pairs, each with distinct scores. The model processes both the image and the question concurrently. We leverage a pre-trained MOE model to synthesize features from a comprehensive set of textual and visual tokens. These tokens are encoded by the state-of-the-art Qwen2.5-7B [17] for text and the robust Dino-v2-large [35] for visual data, respectively. Following previous works [40], the aggregated output is then passed to a classifier, which predicts the answer from a pool of 3129 frequently occurring answers. We present our results based on the performance metrics obtained from the test-dev and test-std sets of the dataset. Details of the pretraining data and results Table are provided in the supplementary materials.

Alt-MoE demonstrates outstanding performance. This can be largely attributed to its dual-directional alignment mechanism and the MoE’s ability to capture dependencies across multiple levels of abstraction. Specifically, the bidirectional alignment facilitates more comprehensive understanding by allowing the model to process both image-to-question and question-to-image, ensuring that contextual and semantic nuances are preserved in both directions. Additionally, the MoE framework enhances this process by distributing the task across specialized experts, each focusing on different levels of abstraction—from object-level details to higher-level semantic reasoning. This layered reasoning capability significantly boosts the model’s performance in complex VQA tasks.

Method	Clotho						Audiocaps					
	Audio → Text			Text → Audio			Audio → Text			Text → Audio		
	R@1	R@5	R@10									
AVFIC [34]	-	-	-	3.0	-	17.5	-	-	-	8.7	-	37.7
ImageBind [13]	-	-	-	6.0	-	28.4	-	-	-	9.3	-	42.3
VALOR [5]	-	-	-	8.4	-	-	-	-	-	-	-	-
LanguageBind [47]	16.1	39.9	53.2	15.5	38.6	51.7	17.8	47.3	64.0	16.5	48.7	64.6
<b>Alt-MoE</b>	17.0	40.8	53.0	20.1	45.2	58.7	20.4	50.8	66.6	19.8	51.4	66.8

Table 2. Zero-shot Performance on Clotho and Audiocaps datasets.

Model	Accuracy (%)	Precision (%)	Recall (%)	F1 Score (%)
CLIP-ViT [37]	82.1	82.4	82.0	82.0
DinoV2 [35]	83.2	83.5	83.3	83.1
<b>Alt-MoE</b>	86.6	86.9	86.6	86.5

Table 3. Comparison of Classification Performance on the ImageNet-1K Dataset.

## 5.5. Image Classification

To clearly demonstrate the ability of multi-directional MoE to integrate existing knowledge and support hierarchical abstract reasoning, we designed an experiment that combines knowledge from various models trained on unified modalities. This experiment clearly demonstrates how MoE can facilitate complementary knowledge integration across different models. Specifically, DinoV2 [35] is a vision-only model, while CLIP-ViT [37] is a text-guided vision model. These models capture distinct types of information, offering complementary perspectives. To validate this hypothesis, we froze both DinoV2 and CLIP-ViT and extracted different representations for the same image. These representations were then aligned and fused using a MoE, followed by a classification head. As shown in the Table 3, the performance of the jointly trained models exceeds that of either model alone, confirming the complementary nature of their representations. Moreover, the vision-only model outperforms the text-guided vision model, suggesting that the latter may struggle to capture fine-grained details effectively.

## 5.6. Validation of Alignment Objectives

Model	Pred	CL	Image → Text			Text → Image		
			R@1	R@5	R@10	R@1	R@5	R@10
Alt-MoE	✓	×	44.2	86.2	95.6	2.6	12.6	25.1
Alt-MoE	✓	✓	66.1	91.9	96.4	66.2	89.6	99.0

Table 4. Performance comparison of prediction alignment and joint training objectives: Image-Text retrieval with Alt-MoE (Qwen-7b, DinoV2-L) on COCO fine-tuning. CL denotes Contrastive Learning. Pred denotes prediction.

Alt-MoE utilizes the MoE router to automatically select

different experts, optimizing for both objectives. This approach helps decouple modality-specific information from shared information, potentially improving the balance between capturing unique modal features and cross-modal relationships. To validate this conclusion, we applied the predicted representations to retrieval tasks. The results in Table 4 indicate that training solely on the prediction alignment objective yields significantly lower performance compared to jointly training on both prediction and contrastive learning objectives. By jointly optimizing for prediction and contrastive learning, the model maximizes the mutual information, while minimizing the conditional entropy. This ensures that Alt-MoE capture the most relevant and informative features, leading to better alignment and retrieval performance. The mutual reinforcement of the two tasks helps in effectively balancing the trade-off between capturing modality-specific features and learning cross-modal relationships.

## 5.7. Ablation Study

Model	MLP	MoE	ALT	Image → Text			Text → Image		
				R@1	R@5	R@10	R@1	R@5	R@10
Alt-MoE	✓	×	✓	74.4	86.0	92.2	82.3	89.5	92.6
Alt-MoE	×	✓	×	68.2	68.7	81.1	74.2	88.7	92.4
Alt-MoE	×	✓	✓	88.1	99.4	99.8	90.1	99.6	99.9

Table 5. Ablation Study of Image-Text Retrieval with the Alt-MoE contrastive learning representations (Qwen-7b, DinoV2-L) on COCO Fine-Tuning.

To validate its effectiveness, we conducted ablation experiments by replacing MoE with MLP and comparing the results. Additionally, we examined the impact of alternating optimization versus non-alternating optimization. As shown in Table 5, indicate that replacing MoE with MLP leads to a significant drop in performance, demonstrating the critical role of MoE. Furthermore, the comparison between alternating optimization and non-alternating optimization reveals that alternating optimization contributes to better model performance.

## 6. Conclusion

In this study, we introduced Alt-MoE, a novel modality-agnostic training strategy and architecture designed for multi-modal learning. Alt-MoE effectively integrates high-performance uni-modal models using bidirectional alignment module, facilitating the alignment of modality pairs in multiple directions and enabling generalization to new tasks and modalities. To validate the modality and task scalability of Alt-MoE, we conducted extensive experiments focused on alignment performance. The experimental results demonstrate that Alt-MoE can easily generalize to new modalities, tasks, and datasets while maintaining the same training strategy and architecture.

## References

- [1] Hassan Akbari, Dan Kondratyuk, Yin Cui, Rachel Hornung, Huisheng Wang, and Hartwig Adam. Alternating gradient descent and mixture-of-experts for integrated multimodal perception. *Advances in Neural Information Processing Systems*, 36:79142–79154, 2023. 3
- [2] Jean-Baptiste Alayrac, Jeff Donahue, Pauline Luc, Antoine Miech, Iain Barr, Yana Hasson, Karel Lenc, Arthur Mensch, Katherine Millican, Malcolm Reynolds, et al. Flamingo: a visual language model for few-shot learning. *Advances in neural information processing systems*, 35:23716–23736, 2022. 3
- [3] Stanislaw Antol, Aishwarya Agrawal, Jiasen Lu, Margaret Mitchell, Dhruv Batra, C. Lawrence Zitnick, and Devi Parikh. VQA: Visual Question Answering. In *International Conference on Computer Vision (ICCV)*, 2015. 6
- [4] Hangbo Bao, Wenhui Wang, Li Dong, Qiang Liu, Owais Khan Mohammed, Kriti Aggarwal, Subhojit Som, and Furu Wei. Vlmo: Unified vision-language pre-training with mixture-of-modality-experts. *arXiv preprint arXiv:2111.02358*, 2021. 1
- [5] Sihan Chen, Xingjian He, Longteng Guo, Xinxin Zhu, Weining Wang, Jinhui Tang, and Jing Liu. Valor: Vision-audio-language omni-perception pretraining model and dataset. *arXiv preprint arXiv:2304.08345*, 2023. 8
- [6] Yen-Chun Chen, Linjie Li, Licheng Yu, Ahmed El Kholy, Faisal Ahmed, Zhe Gan, Yu Cheng, and Jingjing Liu. Uniter: Universal image-text representation learning. In *European conference on computer vision*, pages 104–120. Springer, 2020. 3, 7
- [7] Gerson H Cohen. Align: a program to superimpose protein coordinates, accounting for insertions and deletions. *Journal of applied crystallography*, 30(6):1160–1161, 1997. 7
- [8] Anna Dawid and Yann LeCun. Introduction to latent variable energy-based models: a path toward autonomous machine intelligence. *Journal of Statistical Mechanics: Theory and Experiment*, 2024(10):104011, 2024. 1
- [9] Jia Deng, Wei Dong, Richard Socher, Li-Jia Li, Kai Li, and Li Fei-Fei. Imagenet: A large-scale hierarchical image database. In *2009 IEEE Conference on Computer Vision and Pattern Recognition*, pages 248–255, 2009. 6
- [10] Soham Deshmukh, Benjamin Elizalde, and Huaming Wang. Audio retrieval with wavtext5k and clap training. *arXiv preprint arXiv:2209.14275*, 2022.
- [11] Konstantinos Drossos, Samuel Lipping, and Tuomas Virtanen. Clotho: An audio captioning dataset. In *ICASSP 2020-2020 IEEE International Conference on Acoustics, Speech and Signal Processing (ICASSP)*, pages 736–740. IEEE, 2020. 6
- [12] Frederic Font, Gerard Roma, and Xavier Serra. Freesound technical demo. In *Proceedings of the 21st ACM international conference on Multimedia*, pages 411–412, 2013.
- [13] Rohit Girdhar, Alaaeldin El-Nouby, Zhuang Liu, Mannat Singh, Kalyan Vasudev Alwala, Armand Joulin, and Ishan Misra. Imagebind: One embedding space to bind them all. In *Proceedings of the IEEE/CVF Conference on Computer*

- Vision and Pattern Recognition*, pages 15180–15190, 2023. 1, 8
- [14] Yash Goyal, Tejas Khot, Douglas Summers-Stay, Dhruv Batra, and Devi Parikh. Making the v in vqa matter: Elevating the role of image understanding in visual question answering. In *Proceedings of the IEEE conference on computer vision and pattern recognition*, pages 6904–6913, 2017. 7
- [15] Edward J Hu, Yelong Shen, Phillip Wallis, Zeyuan Allen-Zhu, Yuanzhi Li, Shean Wang, Lu Wang, and Weizhu Chen. Lora: Low-rank adaptation of large language models. *arXiv preprint arXiv:2106.09685*, 2021.
- [16] Minyoung Huh, Brian Cheung, Tongzhou Wang, and Phillip Isola. The platonic representation hypothesis. *arXiv preprint arXiv:2405.07987*, 2024. 3
- [17] Binyuan Hui, Jian Yang, Zeyu Cui, Jiayi Yang, Dayiheng Liu, Lei Zhang, Tianyu Liu, Jiajun Zhang, Bowen Yu, Keming Lu, et al. Qwen2. 5-coder technical report. *arXiv preprint arXiv:2409.12186*, 2024. 7
- [18] Chao Jia, Yinfei Yang, Ye Xia, Yi-Ting Chen, Zarana Parekh, Hieu Pham, Quoc Le, Yun-Hsuan Sung, Zhen Li, and Tom Duerig. Scaling up visual and vision-language representation learning with noisy text supervision. In *International conference on machine learning*, pages 4904–4916. PMLR, 2021. 3
- [19] Peng Jin, Bo Zhu, Li Yuan, and Shuicheng Yan. Moh: Multi-head attention as mixture-of-head attention. *arXiv preprint arXiv:2410.11842*, 2024.
- [20] Chris Dongjoo Kim, Byeongchang Kim, Hyunmin Lee, and Gunhee Kim. AudioCaps: Generating captions for audios in the wild. In *Proceedings of the 2019 Conference of the North American Chapter of the Association for Computational Linguistics: Human Language Technologies, Volume 1 (Long and Short Papers)*, pages 119–132, Minneapolis, Minnesota, 2019. Association for Computational Linguistics. 6
- [21] Ranjay Krishna, Yuke Zhu, Oliver Groth, Justin Johnson, Kenji Hata, Joshua Kravitz, Stephanie Chen, Yannis Kalantidis, Li-Jia Li, David A. Shamma, Michael S. Bernstein, and Fei-Fei Li. Visual genome: Connecting language and vision using crowdsourced dense image annotations, 2016.
- [22] Yann LeCun. A path towards autonomous machine intelligence version 0.9. 2, 2022-06-27. *Open Review*, 62(1):1–62, 2022. 1
- [23] Chunyuan Li, Cliff Wong, Sheng Zhang, Naoto Usuyama, Haotian Liu, Jianwei Yang, Tristan Naumann, Hoifung Poon, and Jianfeng Gao. Llava-med: Training a large language-and-vision assistant for biomedicine in one day. *Advances in Neural Information Processing Systems*, 36, 2024. 3
- [24] Junnan Li, Ramprasaath Selvaraju, Akhilesh Gotmare, Shafiq Joty, Caiming Xiong, and Steven Chu Hong Hoi. Align before fuse: Vision and language representation learning with momentum distillation. *Advances in neural information processing systems*, 34:9694–9705, 2021. 3, 7
- [25] Junnan Li, Dongxu Li, Caiming Xiong, and Steven Hoi. Blip: Bootstrapping language-image pre-training for unified vision-language understanding and generation. In *International conference on machine learning*, pages 12888–12900. PMLR, 2022. 1, 3, 7
- [26] Junnan Li, Dongxu Li, Silvio Savarese, and Steven Hoi. Blip-2: Bootstrapping language-image pre-training with frozen image encoders and large language models. In *International conference on machine learning*, pages 19730–19742. PMLR, 2023. 2, 3, 7
- [27] Xiujun Li, Xi Yin, Chunyuan Li, Pengchuan Zhang, Xiaowei Hu, Lei Zhang, Lijuan Wang, Houdong Hu, Li Dong, Furu Wei, et al. Oscar: Object-semantics aligned pre-training for vision-language tasks. In *Computer Vision–ECCV 2020: 16th European Conference, Glasgow, UK, August 23–28, 2020, Proceedings, Part XXX 16*, pages 121–137. Springer, 2020. 3, 7
- [28] Valerii Likhoshesterov, Anurag Arnab, Krzysztof Choromanski, Mario Lucic, Yi Tay, Adrian Weller, and Mostafa Dehghani. Polyvit: Co-training vision transformers on images, videos and audio. *arXiv preprint arXiv:2111.12993*, 2021. 3
- [29] Bin Lin, Bin Zhu, Yang Ye, Munan Ning, Peng Jin, and Li Yuan. Video-llava: Learning united visual representation by alignment before projection. *arXiv preprint arXiv:2311.10122*, 2023. 3
- [30] Bin Lin, Zhenyu Tang, Yang Ye, Jiayi Cui, Bin Zhu, Peng Jin, Junwu Zhang, Munan Ning, and Li Yuan. Moe-llava: Mixture of experts for large vision-language models. *arXiv preprint arXiv:2401.15947*, 2024. 3
- [31] Tsung-Yi Lin, Michael Maire, Serge Belongie, James Hays, Pietro Perona, Deva Ramanan, Piotr Dollár, and C Lawrence Zitnick. Microsoft coco: Common objects in context. In *Computer Vision–ECCV 2014: 13th European Conference, Zurich, Switzerland, September 6-12, 2014, Proceedings, Part V 13*, pages 740–755. Springer, 2014. 6
- [32] Tsung-Yi Lin, Michael Maire, Serge Belongie, Lubomir Bourdev, Ross Girshick, James Hays, Pietro Perona, Deva Ramanan, C. Lawrence Zitnick, and Piotr Dollár. Microsoft coco: Common objects in context, 2015.
- [33] Haotian Liu, Chunyuan Li, Qingyang Wu, and Yong Jae Lee. Visual instruction tuning. *Advances in neural information processing systems*, 36, 2024. 1, 2, 3
- [34] Arsha Nagrani, Paul Hongsuck Seo, Bryan Seybold, Anja Hauth, Santiago Manen, Chen Sun, and Cordelia Schmid. Learning audio-video modalities from image captions. In *European Conference on Computer Vision*, pages 407–426. Springer, 2022. 8
- [35] Maxime Oquab, Timothée Darcet, Théo Moutakanni, Huy Vo, Marc Szafraniec, Vasil Khalidov, Pierre Fernandez, Daniel Haziza, Francisco Massa, Alaaeldin El-Nouby, et al. Dinov2: Learning robust visual features without supervision. *arXiv preprint arXiv:2304.07193*, 2023. 2, 3, 7, 8
- [36] Bryan A Plummer, Liwei Wang, Chris M Cervantes, Juan C Caicedo, Julia Hockenmaier, and Svetlana Lazebnik. Flickr30k entities: Collecting region-to-phrase correspondences for richer image-to-sentence models. In *Proceedings of the IEEE international conference on computer vision*, pages 2641–2649, 2015. 6
- [37] Alec Radford, Jong Wook Kim, Chris Hallacy, Aditya Ramesh, Gabriel Goh, Sandhini Agarwal, Girish Sastry, Amanda Askell, Pamela Mishkin, Jack Clark, et al. Learning transferable visual models from natural language supervi-

- sion. In *International conference on machine learning*, pages 8748–8763. PMLR, 2021. [1](#), [3](#), [7](#), [8](#)
- [38] Alane Suhr, Stephanie Zhou, Ally Zhang, Iris Zhang, Huajun Bai, and Yoav Artzi. A corpus for reasoning about natural language grounded in photographs, 2019. [6](#)
- [39] Peng Wang, An Yang, Rui Men, Junyang Lin, Shuai Bai, Zhikang Li, Jianxin Ma, Chang Zhou, Jingren Zhou, and Hongxia Yang. Ofa: Unifying architectures, tasks, and modalities through a simple sequence-to-sequence learning framework. In *International conference on machine learning*, pages 23318–23340. PMLR, 2022.
- [40] Peng Wang, Shijie Wang, Junyang Lin, Shuai Bai, Xiaohuan Zhou, Jingren Zhou, Xinggang Wang, and Chang Zhou. One-peace: Exploring one general representation model toward unlimited modalities. *arXiv preprint arXiv:2305.11172*, 2023. [1](#), [7](#)
- [41] Wenhui Wang, Hangbo Bao, Li Dong, Johan Bjorck, Zhiliang Peng, Qiang Liu, Kriti Aggarwal, Owais Khan Mohammed, Saksham Singhal, Subhojit Som, et al. Image as a foreign language: Beit pretraining for all vision and vision-language tasks. *arXiv preprint arXiv:2208.10442*, 2022. [1](#), [7](#)
- [42] Lewei Yao, Runhui Huang, Lu Hou, Guansong Lu, Minzhe Niu, Hang Xu, Xiaodan Liang, Zhenguo Li, Xin Jiang, and Chunjing Xu. Filip: Fine-grained interactive language-image pre-training. *arXiv preprint arXiv:2111.07783*, 2021. [1](#), [7](#)
- [43] Jiahui Yu, Zirui Wang, Vijay Vasudevan, Legg Yeung, Mojtaba Seyedhosseini, and Yonghui Wu. Coca: Contrastive captioners are image-text foundation models. *arXiv preprint arXiv:2205.01917*, 2022.
- [44] Lu Yuan, Dongdong Chen, Yi-Ling Chen, Noel Codella, Xiyang Dai, Jianfeng Gao, Houdong Hu, Xuedong Huang, Boxin Li, Chunyuan Li, et al. Florence: A new foundation model for computer vision. *arXiv preprint arXiv:2111.11432*, 2021. [7](#)
- [45] Duzhen Zhang, Yahan Yu, Chenxing Li, Jiahua Dong, Dan Su, Chenhui Chu, and Dong Yu. Mm-llms: Recent advances in multimodal large language models. *arXiv preprint arXiv:2401.13601*, 2024. [3](#)
- [46] Pengchuan Zhang, Xiujun Li, Xiaowei Hu, Jianwei Yang, Lei Zhang, Lijuan Wang, Yejin Choi, and Jianfeng Gao. Vinvl: Revisiting visual representations in vision-language models. In *Proceedings of the IEEE/CVF conference on computer vision and pattern recognition*, pages 5579–5588, 2021. [7](#)
- [47] Bin Zhu, Bin Lin, Munan Ning, Yang Yan, Jiayi Cui, Hongfa Wang, Yatian Pang, Wenhao Jiang, Junwu Zhang, Zongwei Li, et al. Languagebind: Extending video-language pretraining to n-modality by language-based semantic alignment. *arXiv preprint arXiv:2310.01852*, 2023. [1](#), [8](#)

# Alt-MoE: A Scalable Framework for Bidirectional Multimodal Alignment and Efficient Knowledge Integration

## Supplementary Material

### 1. Appendix

#### 1.1. Experimental Datasets

##### 1. Image-text retrieval datasets:

- COCO [16]: 330,000 images with object annotations and captions, providing a rich resource for multi-label image classification and visual understanding.
- Flickr30K [18]: 30,000 images with descriptive sentences, capturing a diverse range of real-world scenarios.

##### 2. Zero-shot Audio-text Retrieval:

In the zero-shot audio-text task, we trained Alt-MoE on a pretraining dataset and evaluated its performance on unseen datasets. The details of the data are as follows:

- Clotho [6]: 4,981 audio samples with 24,905 descriptions, sourced from the Freesound platform and crowdsourced from English-speaking contributors.
- Audiocaps [11]: A curated subset of AudioSet, focusing on audio captions and enabling the study of audio-text relationships.
- Wavtext5k [5]: The WavText5K data was sourced from two main website: BigSoundBank and and SoundBible 3 (details can be found in [5]). WavText5K contains 4505 audios, 4348 descriptions, 4525 audio titles and 2058 tags.
- Freesound[7]: The Freesound dataset contains 363,618 samples, totaling 2,162.10 hours of audio.

Alt-MoE was tested on the Clotho dataset and trained on AudioCaps, WavText5K, and Freesound. Alt-MoE was tested on the AudioCaps dataset and trained on Clotho, WavText5K, and Freesound.

##### 3. VQA:

- VQA v2 [2]: 265,016 images with multiple questions per image, assessing the ability of models to understand and answer questions about visual content.
- NLVR-2 [19]: 107,292 pairs of images with corresponding sentences, testing the visual reasoning capabilities of models.

##### 4. Image Classification:

- ImageNet 1k [4]: 1,281,167 training images, 50,000 validation images, and 100,000 test images across 1,000 classes, serving as a benchmark for image classification models.

### 1.2. Implementation Details

#### 1.2.1. Zero-shot Audio-text Retrieval

In the zero-shot audio-text retrieval task, we fine-tuned the audio and text encoders from LanguageBind [24]. Alt-MoE was trained on multiple datasets and tested on unseen data to evaluate its generalization capability. The multi-directional MoE uses 12 experts with a top-4 gating ( $k = 4$ ) setting, a configured hidden size of 2048, and a configured dropout rate of 0.1. It is worth noting that we tested LanguageBind under the same settings, and the results are shown in the Table 2.

#### 1.2.2. Visual Question Answer

Specifically, we follow previous work [3, 21, 22] to conduct finetuning experiments on the VQA v2.0 dataset and formulate the task as a classification problem. The task requires the model to answer natural language questions about input images. Alt-MoE’s training strategy adopts a retrieval-based VQA approach, predicting answers from the 3,129 most frequent answer candidates in the training set. For the VQA task, we first perform an alternating alignment task with Alt-MoE on the COCO dataset. We fine-tuned the pretrained multi-directional MoE and applied LoRA [8] to both the vision and language models separately. The vision model uses DinoV2-Large, while the language model is based on Qwen-2.5 [9]. The multi-directional MoE uses 12 experts with a top-4 gating ( $k = 4$ ) setting, a configured hidden size of 2048, and a configured dropout rate of 0.1. Our results on two tasks are lower than BEiT3 and ONE-PEACE (shown in Tabel 1). It is important to highlight that our model was trained exclusively on the VQA v2 training set, whereas other studies have incorporated additional datasets or pretrained on in-domain datasets to boost their model’s performance (such as ONE-PEACE trained with Visual Genome[12],and BEiT-3 pretrained on MSCOCO[17] and Visual Genome).

#### 1.2.3. Image Classification

To thoroughly evaluate the quality of the learned representations, we follow the widely adopted linear probing protocol, where a linear classifier is trained on top of the frozen features to perform classification tasks. We evaluate Alt-MoE, Dino V2, and CLIP-ViT under the same settings on ImageNet-1K. Specifically, Alt-MoE aggregates the representations of Dino V2 and CLIP-ViT using a multi-directional MoE mechanism and is evaluated via linear probing. Notably, with Dino V2 and CLIP-ViT kept frozen,

Method	VQA		NLVR-2	
	test-dev	test-std	dev	test-P
ALBEF [13]	75.8	76.0	82.55	83.14
BLIP [14]	78.25	78.32	82.15	82.24
X-VLM	78.22	78.37	84.41	84.76
SimVLM	80.0	80.3	84.5	85.2
OFA [20]	82.0	82.0	-	-
Flamingo [1]	82.0	82.1	-	-
CoCa [23]	82.3	82.3	86.1	87.0
BLIP-2 [15]	82.2	82.3	-	-
BEIT-3 [22]	<b>84.2</b>	<b>84.0</b>	<b>91.5</b>	<b>92.6</b>
ONE-PEACE [21]	82.6	82.5	87.8	88.3
<b>Alt-MoE</b>	82.3	82.5	86.8	87.6

Table 1. Experimental results on Visual Question Answer.

Alt-MoE achieves the best performance. The MoE is configured with 8 expert heads, a top-k selection of 4, a dropout rate of 0.1, and a hidden size of 2056.

#### 1.2.4. Detail of Multi-directional MoE

The Multi-directional MoE assigns  $k$  experts by applying a softmax function to the input cross-embedding and representation of input modality. Based on our experimental findings, we opted not to include a load-balancing loss in this framework. We tailored the number of experts and the value of  $k$  for each task, optimizing performance. Detailed configurations for different tasks are provided in the supplementary material. The final design of the multi-directional MoE enables the model to perform various tasks based on different modality and embedding cues.

To ensure stable training of sparse-gated MoE under alternating optimization, we experimented with several methods: 1. Random Selection Based on Fixed Probability: We set a probability of 0.5 for both image-to-text and text-to-image tasks, randomly selecting between them. 2. Dynamic Probability Selection: Probabilities were dynamically adjusted based on evaluation results from the validation set. For example, if image-to-text outperformed text-to-image, we increased the probability for text-to-image tasks. 3. Sequential Alternation: Image-to-text and text-to-image tasks were executed in a fixed sequential order. Experimental results showed that the sequential alternation method outperformed the others.

### 1.3. Sensitivity Analysis of Loss Weights

As shown in Figure 1, we experimented with different weight configurations for the contrastive learning loss and the prediction loss to analyze their impact on performance. The y-axis represents the Average Recall@1, while the x-axis indicates the varying loss weights.

From the plot, we observe the following trends: (1) Increasing the contrastive learning weight leads to a steady improvement in Average Recall@1, with performance

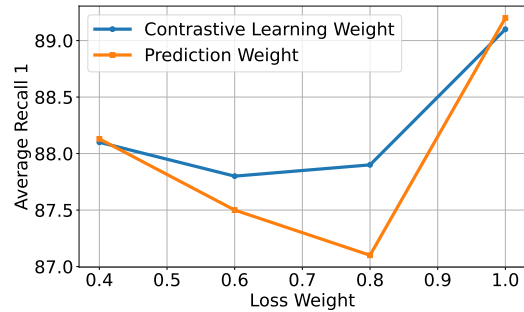


Figure 1. Sensitivity Analysis of Loss Weights

peaking when the weight reaches 1.0. (2) On the other hand, increasing the prediction loss weight initially results in a performance drop, hitting a minimum before recovering as the weight approaches 1.0.

This sensitivity analysis highlights the trade-off between the two loss components. Balancing these weights is crucial, as overemphasizing one can negatively affect the model’s overall retrieval performance. Interestingly, the results suggest that a higher emphasis on contrastive learning contributes more significantly to performance gains in this setting.

### 1.4. Ablation of Modality Encoder Finetuning

Model	Image → Text			Text → Image		
	R@1	R@5	R@10	R@1	R@5	R@10
Alt-MoE(freeze)	75.4	88.6	94.53	84.3	90.1	97.8
Alt-MoE( $N$ layers LoRA)	88.1	<b>99.4</b>	99.8	90.1	99.6	<b>99.9</b>
Alt-MoE(full layer LoRA)	<b>92.1</b>	<b>99.4</b>	<b>99.9</b>	<b>91.1</b>	<b>99.8</b>	<b>99.9</b>

Table 2. Ablation of Modality Encoder Finetuning

The Alt-MoE model’s performance significantly improves with the application of LoRA (Low-Rank Adaptation), particularly with full layer LoRA. The Alt-MoE model with full layer LoRA achieves the highest recall rates across all metrics, with R@1, R@5, and R@10 reaching 92.1%, 99.4%, and 99.9% for Image-to-Text retrieval, and 91.1%, 99.8%, and 99.9% for Text-to-Image retrieval. This demonstrates that full layer LoRA finetuning is the most effective, surpassing both the frozen and partial layer LoRA configurations.

Here, we achieved better results by using Qwen2 and Dino-large with LoRA applied to all layers. However, due to time constraints, we were only able to perform ablation studies with applied LoRA to last three layers of Llama and other models. To ensure a fair comparison, we only included the results of Qwen2 with the last three layers finetuned in the main text.

## 1.5. Retrieval Efficiency

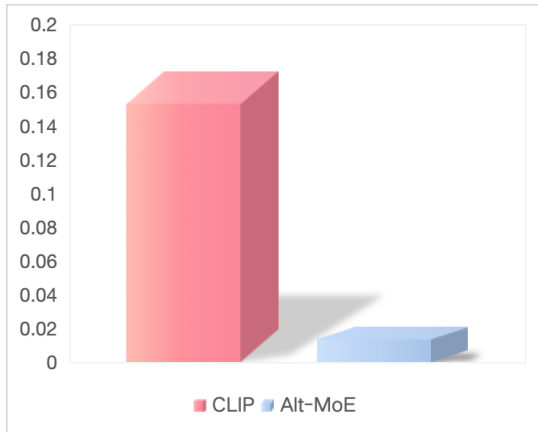


Figure 2. Compare the retrieval efficiency of CLIP and Alt-MoE.

Alt-MoE operates in latent space, supporting vector pre-storage and real-time retrieval via lightweight multi-directional MoE, thereby facilitating massive data processing.

To validate the efficiency of the retrieval, we compared Alt-MoE with the classic dual-encoder model CLIP. The figure 2 shows the retrieval time for a single sample using Alt-MoE and CLIP. As shown in Figure 1, our retrieval time is significantly lower than that of CLIP.

## 1.6. Visualization of the Similarity Matrix

In the experiment, we conducted an image-text retrieval task. The results showed that Alt-MoE performed well in this task, effectively finding matching image-text pairs from a large dataset. To more intuitively demonstrate the model’s performance, we visualized the similarity matrix for 10 text-image pairs from the COCO dataset, for the example purpose. Figure 2 shows our method can differentiate the positive and negative pairs well, which ensures the retrieval performance.

## 1.7. Limitation

In this experiment, we demonstrate the effectiveness of the model across three key tasks: cross-modal retrieval, cross-modal question answering, and image classification. However, as a general multi-modal alignment framework, Alt-MoE still faces the following limitations: 1. Multi-task Scaling: The current experiments focus primarily on cross-modal understanding and reasoning tasks, with limited exploration of generative tasks such as generative visual question answering. As a multi-directional connector, Alt-MoE has the potential to integrate with various generative frameworks, including diffusion models and large language models (LLMs). Future work will aim to extend its

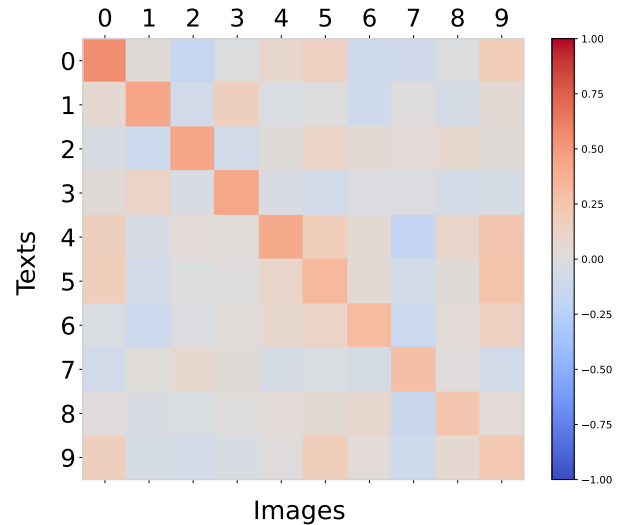


Figure 3. Visualization of the similarity matrix. The up-triangle part indicates text-to-image and the down-triangle part indicates image-to-text. The symmetric line corresponding to the ground truth pairs.

capabilities to multi-modal generation. 2. Modality Expansion: Currently, the framework supports alignment between two modalities. With alternating training, Alt-MoE has the potential to align more than two modalities simultaneously. Further research will explore scaling to more complex multi-modal scenarios. 3. VQA: Although Alt-MoE demonstrates competitive performance in VQA tasks, it does not surpass the current state-of-the-art models. This limitation may stem from the Mixture-of-Experts mechanisms, which may struggle to capture more complex relationships, such as semantic associations and spatial arrangements. While we experimented with local attention mechanisms to aggregate visual semantics, these approaches may not effectively model the global dependencies required for tasks like VQA. Understanding the intricate interplay between questions and image content often requires mechanisms capable of balancing both local and global context. However, the flexibility of the Alt-MoE framework offers opportunities for further enhancements. For instance, incorporating Mixture-of-Heads (MoH) [10] attention mechanisms could improve the model’s ability to represent cross-modal features and better capture semantic and spatial relationships. Future work will focus on implementing and evaluating such enhancements, including the use of MoH and other advanced connection structures, to further improve the model’s performance in VQA and other multi-modal tasks.

## References

- [1] Jean-Baptiste Alayrac, Jeff Donahue, Pauline Luc, Antoine Miech, Iain Barr, Yana Hasson, Karel Lenc, Arthur Mensch, Katherine Millican, Malcolm Reynolds, et al. Flamingo: a visual language model for few-shot learning. *Advances in neural information processing systems*, 35:23716–23736, 2022. 2
- [2] Stanislaw Antol, Aishwarya Agrawal, Jiasen Lu, Margaret Mitchell, Dhruv Batra, C. Lawrence Zitnick, and Devi Parikh. VQA: Visual Question Answering. In *International Conference on Computer Vision (ICCV)*, 2015. 1
- [3] Hangbo Bao, Wenhui Wang, Li Dong, Qiang Liu, Owais Khan Mohammed, Kriti Aggarwal, Subhojit Som, and Furu Wei. Vlm: Unified vision-language pre-training with mixture-of-modality-experts. *arXiv preprint arXiv:2111.02358*, 2021. 1
- [4] Jia Deng, Wei Dong, Richard Socher, Li-Jia Li, Kai Li, and Li Fei-Fei. Imagenet: A large-scale hierarchical image database. In *2009 IEEE Conference on Computer Vision and Pattern Recognition*, pages 248–255, 2009. 1
- [5] Soham Deshmukh, Benjamin Elizalde, and Huaming Wang. Audio retrieval with wavtext5k and clap training. *arXiv preprint arXiv:2209.14275*, 2022. 1
- [6] Konstantinos Drossos, Samuel Lipping, and Tuomas Virtanen. Clotho: An audio captioning dataset. In *ICASSP 2020-2020 IEEE International Conference on Acoustics, Speech and Signal Processing (ICASSP)*, pages 736–740. IEEE, 2020. 1
- [7] Frederic Font, Gerard Roma, and Xavier Serra. Freesound technical demo. In *Proceedings of the 21st ACM international conference on Multimedia*, pages 411–412, 2013. 1
- [8] Edward J Hu, Yelong Shen, Phillip Wallis, Zeyuan Allen-Zhu, Yuanzhi Li, Shean Wang, Lu Wang, and Weizhu Chen. Lora: Low-rank adaptation of large language models. *arXiv preprint arXiv:2106.09685*, 2021. 1
- [9] Binyuan Hui, Jian Yang, Zeyu Cui, Jiayi Yang, Dayiheng Liu, Lei Zhang, Tianyu Liu, Jiajun Zhang, Bowen Yu, Keming Lu, et al. Qwen2. 5-coder technical report. *arXiv preprint arXiv:2409.12186*, 2024. 1
- [10] Peng Jin, Bo Zhu, Li Yuan, and Shuicheng Yan. Moh: Multi-head attention as mixture-of-head attention. *arXiv preprint arXiv:2410.11842*, 2024. 3
- [11] Chris Dongjoo Kim, Byeongchang Kim, Hyunmin Lee, and Gunhee Kim. AudioCaps: Generating captions for audios in the wild. In *Proceedings of the 2019 Conference of the North American Chapter of the Association for Computational Linguistics: Human Language Technologies, Volume 1 (Long and Short Papers)*, pages 119–132, Minneapolis, Minnesota, 2019. Association for Computational Linguistics. 1
- [12] Ranjay Krishna, Yuke Zhu, Oliver Groth, Justin Johnson, Kenji Hata, Joshua Kravitz, Stephanie Chen, Yannis Kalantidis, Li-Jia Li, David A. Shamma, Michael S. Bernstein, and Fei-Fei Li. Visual genome: Connecting language and vision using crowdsourced dense image annotations, 2016. 1
- [13] Junnan Li, Ramprasaath Selvaraju, Akhilesh Gotmare, Shafiq Joty, Caiming Xiong, and Steven Chu Hong Hoi. Align before fuse: Vision and language representation learning with momentum distillation. *Advances in neural information processing systems*, 34:9694–9705, 2021. 2
- [14] Junnan Li, Dongxu Li, Caiming Xiong, and Steven Hoi. Blip: Bootstrapping language-image pre-training for unified vision-language understanding and generation. In *International conference on machine learning*, pages 12888–12900. PMLR, 2022. 2
- [15] Junnan Li, Dongxu Li, Silvio Savarese, and Steven Hoi. Blip-2: Bootstrapping language-image pre-training with frozen image encoders and large language models. In *International conference on machine learning*, pages 19730–19742. PMLR, 2023. 2
- [16] Tsung-Yi Lin, Michael Maire, Serge Belongie, James Hays, Pietro Perona, Deva Ramanan, Piotr Dollár, and C Lawrence Zitnick. Microsoft coco: Common objects in context. In *Computer Vision—ECCV 2014: 13th European Conference, Zurich, Switzerland, September 6–12, 2014, Proceedings, Part V 13*, pages 740–755. Springer, 2014. 1
- [17] Tsung-Yi Lin, Michael Maire, Serge Belongie, Lubomir Bourdev, Ross Girshick, James Hays, Pietro Perona, Deva Ramanan, C. Lawrence Zitnick, and Piotr Dollár. Microsoft coco: Common objects in context, 2015. 1
- [18] Bryan A Plummer, Liwei Wang, Chris M Cervantes, Juan C Caicedo, Julia Hockenmaier, and Svetlana Lazebnik. Flickr30k entities: Collecting region-to-phrase correspondences for richer image-to-sentence models. In *Proceedings of the IEEE international conference on computer vision*, pages 2641–2649, 2015. 1
- [19] Alane Suhr, Stephanie Zhou, Ally Zhang, Iris Zhang, Huajun Bai, and Yoav Artzi. A corpus for reasoning about natural language grounded in photographs, 2019. 1
- [20] Peng Wang, An Yang, Rui Men, Junyang Lin, Shuai Bai, Zhikang Li, Jianxin Ma, Chang Zhou, Jingren Zhou, and Hongxia Yang. Ofa: Unifying architectures, tasks, and modalities through a simple sequence-to-sequence learning framework. In *International conference on machine learning*, pages 23318–23340. PMLR, 2022. 2
- [21] Peng Wang, Shijie Wang, Junyang Lin, Shuai Bai, Xiaohuan Zhou, Jingren Zhou, Xinggang Wang, and Chang Zhou. One-peace: Exploring one general representation model toward unlimited modalities. *arXiv preprint arXiv:2305.11172*, 2023. 1, 2
- [22] Wenhui Wang, Hangbo Bao, Li Dong, Johan Bjorck, Zhiliang Peng, Qiang Liu, Kriti Aggarwal, Owais Khan Mohammed, Saksham Singhal, Subhojit Som, et al. Image as a foreign language: Beit pretraining for all vision and vision-language tasks. *arXiv preprint arXiv:2208.10442*, 2022. 1, 2
- [23] Jiahui Yu, Zirui Wang, Vijay Vasudevan, Legg Yeung, Mojtaba Seyedhosseini, and Yonghui Wu. Coca: Contrastive captioners are image-text foundation models. *arXiv preprint arXiv:2205.01917*, 2022. 2
- [24] Bin Zhu, Bin Lin, Munan Ning, Yang Yan, Jiayi Cui, Hongfa Wang, Yatian Pang, Wenhao Jiang, Junwu Zhang, Zongwei Li, et al. Languagebind: Extending video-language pretraining to n-modality by language-based semantic alignment. *arXiv preprint arXiv:2310.01852*, 2023. 1